Global and Planetary Change 164 (2018) 1–10

Contents lists available at ScienceDirect

Global and Planetary Change

journal homepage: www.elsevier.com/locate/gloplacha

On the relationship between the early spring Indian Ocean's sea surface temperature (SST) and the Tibetan Plateau atmospheric heat source in summer

Chenxu Ji[a], Yuanzhi Zhang[a,b,*], Qiuming Cheng[c,**], Yu Li[d], Tingchen Jiang[e], X. San Liang[a]

[a] Nanjing University of Information Science and Technology, School of Marine Sciences, Nanjing 210044, China
[b] Chinese University of Hong Kong, Center for Housing Innovations, Shatin, Hong Kong
[c] China University of Geosciences, State Key Laboratory for Geological Processes and Mineral Resources, Beijing 100083, China
[d] Beijing University of Technology, Faculty of Information Science, Beijing 100124, China
[e] Huaihai Institute of Technology, Faculty of Surveying and Mapping, Lianyungang 222005, China

ARTICLE INFO

Editor: Zhengtang Guo

Keywords:
Sea surface temperature (SST)
Heat source
Indian Ocean
Tibetan Plateau
Atmospheric circulation

ABSTRACT

In this study, we evaluated the effects of springtime Indian Ocean's sea surface temperature (SST) on the Tibetan Plateau's role as atmospheric heat source (AHS) in summer. The SST data of the National Oceanic and Atmospheric Administration (NOAA), European Centre for Medium-Range Weather Forecasts (ECMWF) and the Hadley Centre Sea Ice and Sea Surface Temperature data set (HadISST) and the reanalysis data of the National Center for Environmental Prediction (NCEP) and National Center for Atmospheric Research (NCAR) for 33 years (from 1979 to 2011) were used to analyze the relationship between the Indian Ocean SST and the Tibetan Plateau's AHS in summer, using the approaches that include correlation analysis, and lead–lag analysis. Our results show that some certain strong oceanic SSTs affect the summer plateau heat, specially finding that the early spring SSTs of the Indian Ocean significantly affect the plateau's ability to serve as a heat source in summer. Moreover, the anomalous atmospheric circulation and transport of water vapor are related to the Plateau heat variation.

1. Introduction

Known as the “roof of the world,” the Tibetan Plateau (hereinafter the plateau) sits at an average altitude of 4000 m, making it the world's highest plateau. As a heat island on the Eurasian continent, the plateau has always been an important topic within the realm of meteorological research for its thermal state.

Ground-to-atmosphere heat transfer is mainly achieved through radiative, latent, and sensible heating—all of which, being diabatic heating sources, are the driving force of atmospheric circulation; accordingly, their evolution contributes greatly to circulation over the plateau. Naturally, the plateau features differences in surface heating throughout the year—with, for example, sensible heat being the main contributor in spring. As a result, the plateau acts as a “heat pump” (Wu et al., 1997) regulating atmospheric motion throughout Asia (Wu and Zhang, 1998). At the same time, it plays an important role in deciding the climate of the entire Northern Hemisphere (Tao and Ding, 1981). In summer, by contrast, latent heating dominates. Various studies have reported that the plateau's role as heat source has affected as well as been affected by climate decadal change and even global climate change (Zou and Zhao, 2008; Cai et al., 2008).

China, being located in the classic Asian monsoon region, is affected by the monsoon's seasonal change. Moreover, differences in the thermodynamic properties of the sea and the land fundamentally affect the formation of the monsoon. To begin with, the sea surface temperature (SST) of the tropical Pacific Ocean influences the plateau's climate, which also derives from various air–sea interactions that are themselves modulated by atmospheric circulation over the ocean. One previous study, applying singular value decomposition (SVD) to analyze the plateau's climatic variability and spatial distribution of air temperature from 1960 to 2000 showed that plateau air temperature correlated with the SST of Indian Ocean (Zhang et al., 2006). When reanalyzing surface sensible heat flux data, the spatio-temporal distribution characteristics of global surface sensible heat revealed a significant correlation among the equatorial central Indian Ocean and Northwest Pacific Ocean SSTs and surface sensible heat anomalies over the plateau (Zhang and Qian,

* Correspondence to: Y. Zhang, Nanjing University of Information Science and Technology, School of Marine Sciences, Nanjing 210044, China.
** Corresponding author.
E-mail addresses: yuanzhizhang@cuhk.edu.hk (Y. Zhang), qiuming.cheng@iugs.org (Q. Cheng).

https://doi.org/10.1016/j.gloplacha.2018.02.011
Received 19 June 2017; Received in revised form 23 February 2018; Accepted 23 February 2018
Available online 27 February 2018

2004). In addition, reflecting differences between land and sea, the relationship between SST and the Asian monsoon betrays a certain connection—specifically, between the East Pacific SST and the Asian monsoon. Internal relationships can also be traced between monsoon intensity and plateau thermal state (Li and Yanai, 1996).

Latest studies reported that the MLR and PCR models were used to capture the pattern of monsoon rainfall during the training and verification periods, in which the result shows that SST variables play an important role in the prediction of summer monsoon rainfall in Pakistan (Muhammad et al., 2017).

In addition, the South Asian summer monsoon (SASM) displays variability on a range of time scales, from intraseasonal, to decadal—and, indeed, beyond (Webster et al., 1998; Gadgil, 2003; Turner and Annamalai, 2012; Schneider et al., 2014). Traditionally, the SASM has been viewed as a large-scale sea-breeze circulation, driven by surface temperature contrasts and their associated atmospheric pressure gradients between the Asian continent to the north and the Indian Ocean to the south (Webster and Fasullo, 2003). The sea breeze paradigm has been extended to include the effects of elevated diabatic heating from moist convection (Webster et al., 1998) and the Tibetan plateau (Li and Yanai, 1996), which is consistent with some recent observational studies that have shown that interannual variability of the SASM circulation is more strongly correlated with upper-tropospheric thermal contrasts than lower-tropospheric thermal contrasts (Dai et al., 2013; Sun et al., 2010).

Previous studies have speculated that plateau orography could very significantly affect moist static energy distribution, by shielding India and Southeast Asia from inflow from the Asian mid-latitudes, and by strengthening monsoon precipitation and allowing it to extend farther poleward (Privé and Plumb, 2007). However, some scientists have shown, through estimates of meridional temperature advection in a general circulation model (GCM), that orography acts as a barrier for the cold winds from the upper-latitudes (Chakraborty et al., 2006). Using reanalysis, radiosonde, and satellite data, it is found that monsoon strength was, similarly, perturbed little by setting the surface albedo of the plateau to unity, which eliminates the ability of the plateau to serve as a heat source (Boos and Kuang, 2010).

It is suggested that the Mascarene High interacts with the underlying SST anomalies through a positive dynamical feedback mechanism, maintaining its anomalous position during the late Indian summer monsoon (LISM) (Zou and Zhao, 2008). Moreover, the Subtropical Indian Ocean Dipole (SIOD) is closely related to regional sea-air interaction, which can alter heating in the atmosphere of South Asia and tropical Pacific (Terray et al., 2003). This also suggested to cause the Asian summer monsoon and precipitation anomalies (Yang, 2006).

Walker et al. (2015) investigated the interannual variability of precipitation and large-scale dynamics of the SASM and found that there is a negative correlation between the SASM strength and the near-surface thermal contrast between the continent and the Indian Ocean. It suggests that the near-surface atmospheric temperature distribution is itself a response to the atmospheric circulation rather than a forcing factor. Within the SASM sector, teleconnections exist between the monsoon strength and the Southern Hemisphere extratropical atmospheric temperatures, eddy moist static energy (MSE) fluxes, eddy momentum flux divergence (EMFD), and jet structure (Walker et al., 2015).

On the other hand, many scholars noted that the Arctic Oscillation (AO) has a discernible effect on the Plateau temperature (Jiao et al., 2014), and it would affect the January Climate over South China (Yang, 2011). Some studies found that the North Atlantic Oscillation (NAO) could extend its influence downstream to East Asia via the subtropical jet waveguide, as well as that it exerts an even stronger influence on the climate of southwestern China (Li et al., 2008).

Although much research has examined the correlation between SST and plateau temperature, only a few studies have considered SSTs' influence on the plateau's role as atmospheric heat source. Many studies, in particular, have focused only on the area of the Pacific Ocean—but only a few on the Indian Ocean.

This study analyzes the effect of early spring strong SST signals on the plateau's atmospheric heat source in summer, with particular focuses on the relevant characteristics of the atmospheric heat source on the plateau and the Indian Ocean SST, and on the effects of continuous thermal forcing on the Plateau. The spring spatio-temporal SST distribution is also analyzed using National Ocean & Atmospheric Administration (NOAA) datasets.

2. Data and methods

2.1. Data sets

2.1.1. NOAA SST data

Monthly mean SST data were provided by the National Oceanic and Atmospheric Administration (NOAA) from 1979 to 2011, with 180 × 89 grid points and a horizontal resolution of 2.5° × 2.5°.

2.1.2. ERA interim datasets

Monthly means of daily means SST data (https://www.ecmwf.int/) were obtained from European Centre for Medium-Range Weather Forecasts (ECMWF), with a horizontal resolution of 0.75° × 0.75°.

2.1.3. Met Office Hadley Centre observations datasets

The Hadley Centre Sea Ice and Sea Surface Temperature data set (HadISST) were also utilized in this paper. We get the monthly mean SST data with a horizontal resolution of 1° × 1° from (https://www.metoffice.gov.uk/hadobs/hadisst/).

2.1.4. NCEP/NCAR reanalysis data

Daily NCEP/NCAR reanalysis data (http://www.esrl.noaa.gov/psd/) from 1979 to 2011 were used in the study. Variables chosen include geopotential height field (h), temperature field (T), zonal wind (u), and the meridional wind (v), with horizontal resolution at 2.5° × 2.5°, including 17 levels (1000, 925, 850, 700, 600, 500, 400, 300, 250, 200, 150, 100, 70, 50, 30, 20, and 10 hPa).

2.2. Methods

2.2.1. Atmospheric heat source calculation

An atmospheric heat source (sink) is a physical quantity that reflects the heat budget of the air column. For a given region, it is defined as the heat an atmospheric column gained (lost) in a given period of time (Yanai et al., 1973). From the thermodynamic equation, AHS can be denoted as:

$$Q_1 = C_p\left[\frac{\partial \mathrm{T}}{\partial \mathrm{t}} + \overline{V}\bullet\nabla \mathrm{T} + \left(\frac{p}{p_0}\right)^k \omega\frac{\partial\theta}{\partial \mathrm{p}}\right] \tag{1}$$

Eq. (1) can be vertically integrated (Yanai and Li, 1994):

$$\langle Q_1\rangle = \frac{1}{g}\int_{100}^{p_0} Q_1 dp = \frac{C_p}{g}\int_{p_1}^{p_s}\left[\frac{\partial \mathrm{T}}{\partial \mathrm{t}} + \overline{V}\bullet\nabla \mathrm{T} + \left(\frac{p}{p_0}\right)^k \omega\frac{\partial\theta}{\partial \mathrm{p}}\right]dp \tag{2}$$

where Q_1 is the atmospheric heat source (sink) per unit. p_0 = 100 hPa. p_s and p_t are pressures at surface and at top (100 hPa), respectively. T is temperature, V is the horizontal wind vector, p is pressure, and $k = R/C_P$. R and C_P denote the gas constant and specific heat of dry air at constant pressure, respectively. ω is the vertical velocity, θ is potential temperature, L is the latent heat of condensation, P is the precipitation rate, Q_S is the surface sensible heat, and $\langle Q_R\rangle$ represents the vertical integration of radiation heating (cooling). The linear trend was calculated by the least-squares method and the t-test was used to determine the confidence level.

2.2.2. Calculation of standardization index

To eliminate the influence of variation and dimension of variables, the data was standardized by the *Z*-SCORE method. The method is based on the data mean and standard deviation for data standardization, which is called the anomaly index and calculated by Zill et al. (2011):

$$K_i = \frac{X_i - \overline{X}}{S} \quad i = 1, 2, 3.....,n \tag{3}$$

where X_i is the value of a year (month or season), $\overline{X}$ is the mean, and S the standard deviation.

If the absolute value of K_i lies between 0.1 and 1, it is in the normal range. If it is > 1, it is abnormal. If it is > 2, it means that the year's average is much greater than the average value. While it is less than −1, it is on the low side.

2.2.3. Correlation analysis

The Pearson correlation coefficient is used to measure whether there is a linear relationship between the selected variables. The expression is given by Pearson (1895):

$$r = \frac{1}{n-1}\sum_{i=1}^{n}\left(\frac{X_i - \overline{X}}{S_x}\right)\left(\frac{Y_i - \overline{Y}}{S_y}\right) \tag{4}$$

where n is the size of sample X and Y, S_X and S_Y are the standard deviation of X and Y, and $\overline{X}$ and $\overline{Y}$ are the mean value of X and Y, r lies between −1 and 1. If $r > 0$, the two variables are positively correlated. If $r < 0$, the two variables are negatively correlated. It should be noted that there is no causal link between them. If $r = 0$, there is no linear relationship between the variables. But they may be connected by other ways. A *t*-test can be carried out to judge the relevant level.

2.2.4. Mann–Kendall test

The Mann–Kendall test is a statistical test widely used for the analysis of trends in climatologic and hydrologic time series. According to this test, the null hypothesis H_0 assumes that there is no trend (in which the data is independent and randomly ordered) and this is tested against the alternative hypothesis H_1, which assumes that there is a trend. The formula is expressed as (Mann, 1945; Kendall, 1975):

$$Z_c = \begin{cases} \frac{S-1}{\sqrt{var(S)}}, & S > 0 \\ 0, \quad S = 0 \\ \frac{S+1}{\sqrt{var(S)}}, & S < 0 \end{cases} \tag{5}$$

The test statistic Z_c is used as a measure of the significance of a trend. Where S is:

$$S = \sum_{i=1}^{n-1}\sum_{k=i+1}^{n} sgn(x_k - x_i) \tag{6}$$

where, x_k and x_i are the annual values in years k and i, and $k > i$, respectively.

$$var[S] = \left[n(n-1)(2n+5) - \sum_t t(t-1)(2t+5)\right]/18 \tag{7}$$

where t is the number of observations. The summation term in the numerator is used only if the data series contains tied values.

$$\beta = \text{Median}\left(\frac{x_i - x_j}{i - j}\right), \forall\, j < i \tag{8}$$

$1 < j < i < n$, beta is represented by the slope; the positive value rises and negative value declines, thereby the value represents whether the trend is obvious.

When $|Z_c| > 1.96$, it represents that the trend is significant under the confidence of 95%. If $|Z_c| > 2.576$, the trend is more remarkable (under the confidence of 99%).

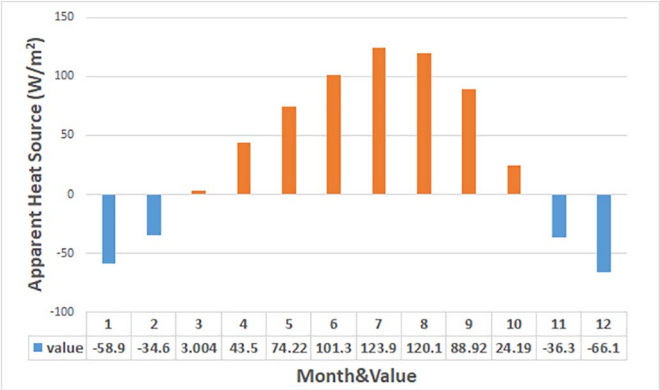

Fig. 1. Monthly average of whole layer atmospheric heat source in the Plateau (1979–2011) (unit: W/m^2).

3. Results and discussion

3.1. Plateau heat source variation

The plateau generally serves as a source of heat in the spring and summer and transfers heat by many forms, including through atmospheric column radiation, surface sensible heat, and condensation latent heat (Wang, 2012). Notable seasonality is reported, with sensible heat reaching its zenith in spring, then decreasing significantly during autumn and winter. Overall, the plateau becomes a heat sink in winter (Wang et al., 2012). In the selected area of 75°–105°E and 28°–38°N, we calculated atmospheric heat source Q_1 using Eq. (2), integrating from 600 hPa to 100 hPa, to reach a value for the entire atmospheric column above the Plateau. Fig. 1 shows the annual cycle of the entire integrated layer from 1979 to 2011. It is clear that the atmosphere above the plateau serves as a heat source in spring, reaches a maximum in summer, and transforms into a cold source in autumn, consistent with the previous results (Zhu et al., 2013).

Fig. 2 shows an overall downward trend of summer-time heat, in which the past five-years' values consistently begin to rise but return to their original value, much as described in Wang et al. (2012). Although the plateau is trending down as a heat source, this trend does not pass the M-K test, with a value of 0.4493 and is not significant. In general, our results agree well with those of previous studies (Duan and Wu, 2008; Wang et al., 2012): plateau atmospheric heat source in the spring, with a downward trend following. As abnormal changes in high altitude heat often lead to changes in atmospheric circulation over the plateau

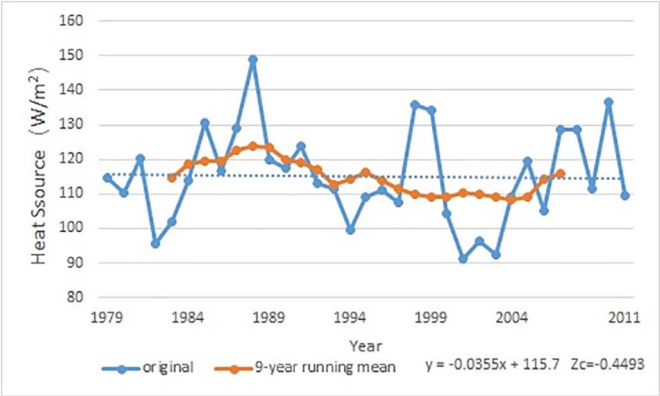

Fig. 2. The long-term variation of the Plateau heat source (blue) and the 9-year running mean (red) in the summers of 1979–2011(unit: W/m^2); $|Z_c| < 1.28$, the download trend is not significant (not pass the M-K test with the confidence of 90%). (For interpretation of the references to colour in this figure legend, the reader is referred to the web version of this article.)

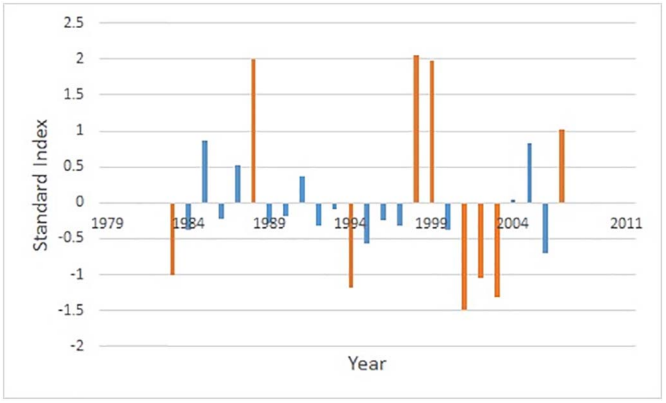

Fig. 3. The normalization index of the original summer Q_1 minus the 9-year running mean.

and the surrounding area, such changes affect both weather and climate.

By removing the interdecadal signals (9-year running mean) from the original whole layer heat source Q_1, the normalization index is calculated as shown in Fig. 3.

Certain inter-annual variations of the plateau as heat source are obvious. Taking $K_i = 1$ as the threshold, the high (low) value of the heat source is immediately apparent. As seen in Fig. 3, abnormally high years were 1988, 1998, 1999, and 2007; abnormally low years were 1983, 1994, 2001, 2002, and 2003.

3.2. SST signals affecting the summer heat source

3.2.1. Plateau summer heat-source and spring-time SST correlations

Using NCEP/NCAR datasets, the plateau's Q_1 is integrated from 600 hPa to 100 hPa. To determine the effect of antecedent SSTs on Q_1 of summer, taking the NOAA's SST for example, the correlation between Q_1 and SST is calculated. Before SST time series correlation analysis, the data were de-trended. This smoothing method eliminated the residual wiggles associated with the imperfect sampling of annual variations without significantly annual variation (Hartmann and Michelsen, 1989).

Fig. 4 shows the correlation coefficient distribution of the plateau Q_1 for summer and antecedent spring SSTs (NOAA's SST data) in the plateau region during the period 1979–2011. Coloured areas represent high correlation between SST field and Q_1, with correlation coefficients passing the *t*-test, with a confidence level of 95%. Table 1 gives the correlation coefficient for each mainly correlated area.

As shown in Fig. 4, five main “strong signals” lie in the Indian Ocean: the areas featuring high levels of correlation of SSTs and Q_1. One negative region is situated in the Southwest Indian Ocean (south of Madagascar, centred at about 100°E and 20°S, marked as area i.1), and the other four positive areas are located in the Southeast Indian Ocean (west of Australia, at 70°–105°E and 50°–20°S, marked as area i.2), west in the Indian Peninsula at 50°–100°E and 10°S–10°N (marked as area i.3), west of Madagascar (marked as area i.4) and northwest of Australia (marked as area i.5). It is clear that the area of i.1 and i.2 has an overlap level the position of Subtropical Indian Ocean Dipole (SIOD). This is featured by the oscillation of SST in which the southwest Indian Ocean (i.e., the south of Madagascar is warmer and then colder than the eastern part, which is off Australia) (Behera and Yamagata, 2001). SIOD-related anomalies over the Southeastern Indian Ocean are also thought to affect the position of the Mascarene High and thus the Indian summer monsoon. Positive (negative) SIOD events during boreal winter are always followed by weak (strong) Indian summer monsoons. During a positive (negative) SIOD events, the Mascarene High shifts southeastward (northwestward) from austral to boreal summer, weakening (strengthening) the monsoon circulation system by modulating the

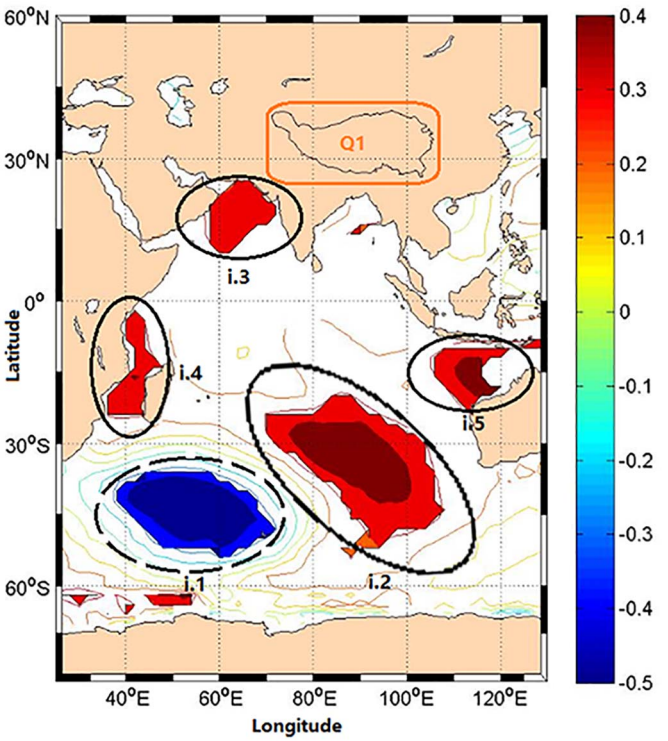

Fig. 4. Correlation between the summer Plateau Q_1 and antecedent Indian Ocean SST for the period of 1979 to 2011 (NOAA's SST; the areas passing 95% significance test are coloured; i.1, i.2, i.3, i.4, and i.5 represent the high correlation areas in the Indian Ocean); before the correlation analysis on the SSTs time series, the data were de-trended.

Table 1
The correlation coefficient of each colour area.

Area	i.1	i.2	i.3	i.4	i.5
March (a)	−0.39	0.38	0.37	0.36	0.38

Note: i.1, i.2, i.3, i.4, and i.5 are the areas of correlation marked in Fig. 4. The coloured areas passed 95% significance testing.

local Hadley cell during the Indian summer monsoon event (Privé and Plumb, 2007).

Then, two major correlated areas of the Indian Ocean selected from Fig. 4 (area: i.2 & i.1) were chosen as an example. For the selected areas, the standard indexes of spring SSTs are calculated by Eq. (3), and presented in Fig. 5. Moreover, the normalized index of summer Q_1 is also shown in the figure. As we can see from the figure, the variation of the SST and Q_1 are almost same in Fig. 5a (the positive correlated area). However, in Fig. 5b, it shows out-of-phase change tendency, which means that the spring-time SST in the area i.1 is negatively correlated with the summer Q_1.

To verify the result in previous paragraphs, the SST data from ECMWF and Hadley Centre are also applied to the correlation analysis. Fig. 6 gives the correlation between the summer Plateau Q_1 and antecedent SST for the period of 1979 to 2011 (Fig. 6a: ERA interim SST; Fig. 6b: HadISST). It is clear that the distribution of related areas in Fig. 6a almost overlap with those in Fig. 4, particularly in the south of the Indian Ocean, north-west of the Pacific Ocean, and the equatorial Atlantic, nearly located in the same position. Comparing Fig. 6b with Fig. 4, the correlated areas of i.1 in Fig. 4 also present in Fig. 6b. This further illustrates that the spring-time Indian Ocean SSTs have impact on the summer Plateau Q_1.

3.2.2. Lead-lag correlations of plateau heat source and Indian Ocean SST

To further analyze the effects of Indian Ocean SST on the persistence

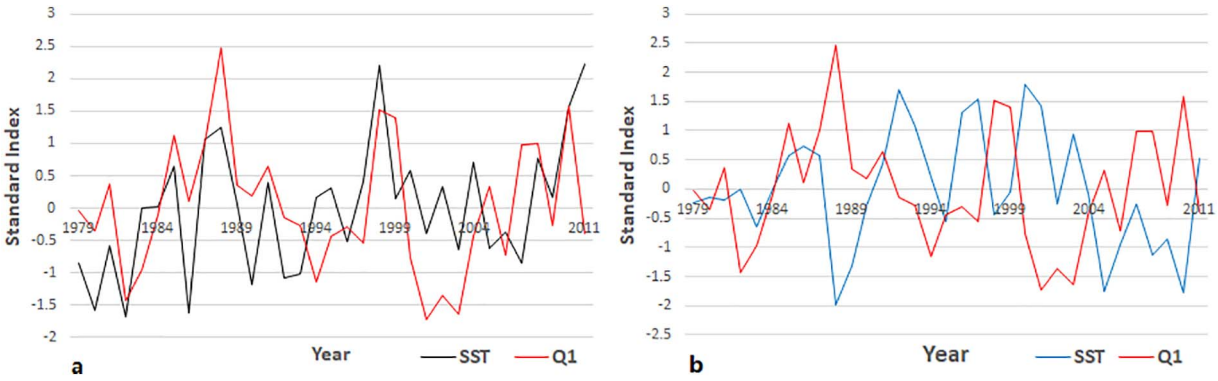

Fig. 5. The normalized index change curve of summer Q_1 and spring Indian Ocean SST of two related section (75°–105°E and 50°–20°S & 40°–60°E and 50°–40°S; 1979–2011): (a) red: Q_1, black: SST in the area of i.2 in Fig. 4, and (b) red: Q_1, blue: SST in the area of i.1 in Fig. 4. (For interpretation of the references to colour in this figure legend, the reader is referred to the web version of this article.)

of the plateau over different periods, we selected June, July and August as relevant months to calculate the correlation coefficient between Q_1 and Indian Ocean SST. According the correlation field was found to be most significant in August.

Fig. 7 shows the distribution of the correlation coefficient between the Q_1 of August and the previous Indian Ocean SSTs of March, April, May, and June, respectively. The colour areas have passed the test at a confidence level of 95%. When considering the Indian Ocean, correlation areas are varying over time. Table 2 gives the correlation coefficient of each correlated area and month. Table 3 is the proportion of each correlated area at different times (unit: ‰).

For the Indian Ocean, the main positive (centred at about 100°E and 20°S, marked as area i.2) and negative (centred at about 60°E and 40°S, marked as area i.1) high-correlation zones diminish with time, and the positive area disappears in May. But as can be seen in Table 3, the coefficient remains nearly the same. That is, the SST of the Indian Ocean in March and April has a significant effect on the plateau Q_1 of August. Regression analysis shows that warm sea temperatures in the Indian Ocean affect atmospheric circulation in East Asia after spring, enhancing the South Asian high as reported by Kang (2009).

Then, two major correlated areas of the Indian Ocean selected from Fig. 7a and b (area: a.i.1 & a.i.2) are chosen as an example. Fig. 8 shows the correlation scatter plot of the spring-time SST and Q_1 in August of two related section (75°–105°E and 50°–20°S & 40°–60°E and 50°–40°S) in the Indian Ocean for 1979–2011. As can be seen in Fig. 8, the plateau heat source is correlated with the SST of the South Indian Ocean.

3.3. Anomalous atmospheric circulation and water vapor flux links to the Plateau heat and Indian Ocean SST

Earth's seasonal cycle of insolation drives monsoon circulations only indirectly, with ocean and land surfaces absorbing most shortwave radiation before transferring the energy of that radiation to the overlying atmosphere via turbulent heat fluxes. It is not surprised that variations in the strength of monsoons have, for more than a century, been associated with changes in the properties of land and ocean surfaces (John and William, 2013; Zhang and Ge, 2013). Plentiful studies show that the atmospheric circulation is associated with the SST (Lau, 1997; Frankignoul and Sennéchael, 2007). What's more, some researchers recently found that the TPSM is associated with the surface sensible

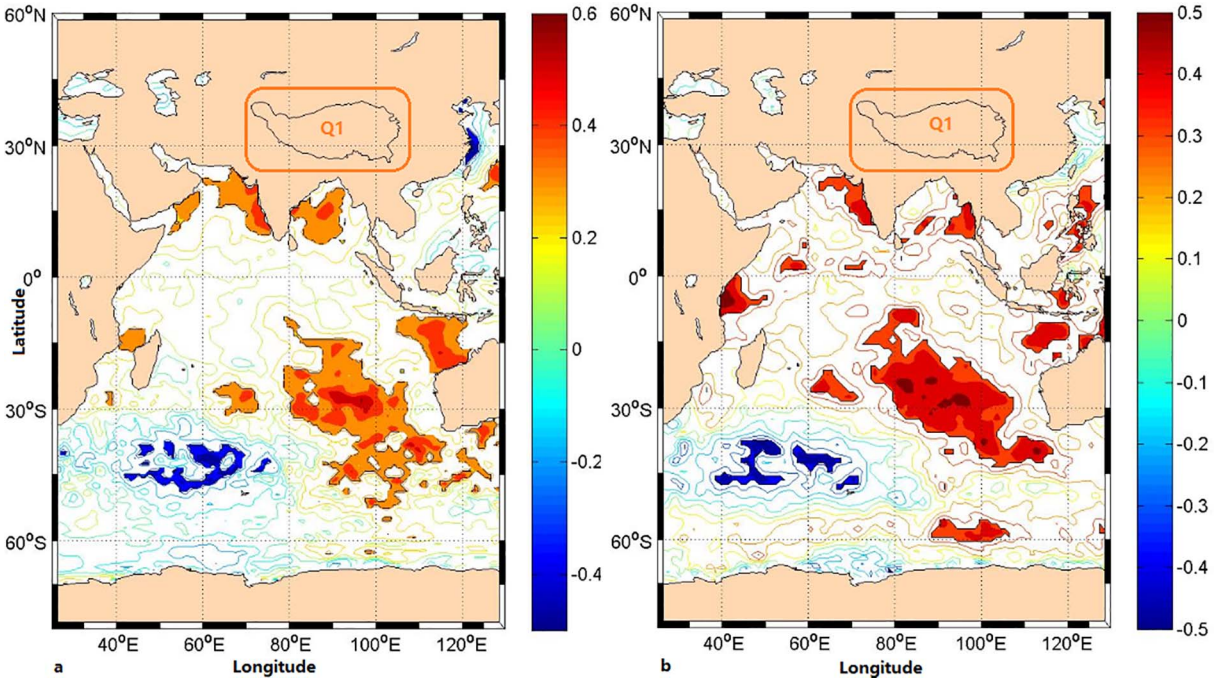

Fig. 6. Correlation between the summer Plateau Q_1 and antecedent Indian Ocean's SSTs for the period of 1979 to 2011 (a: ERA interim SST; b: HadISST), (the areas passing 95% significance test are coloured; before the correlation analysis on the SSTs time series, the data were de-trended).

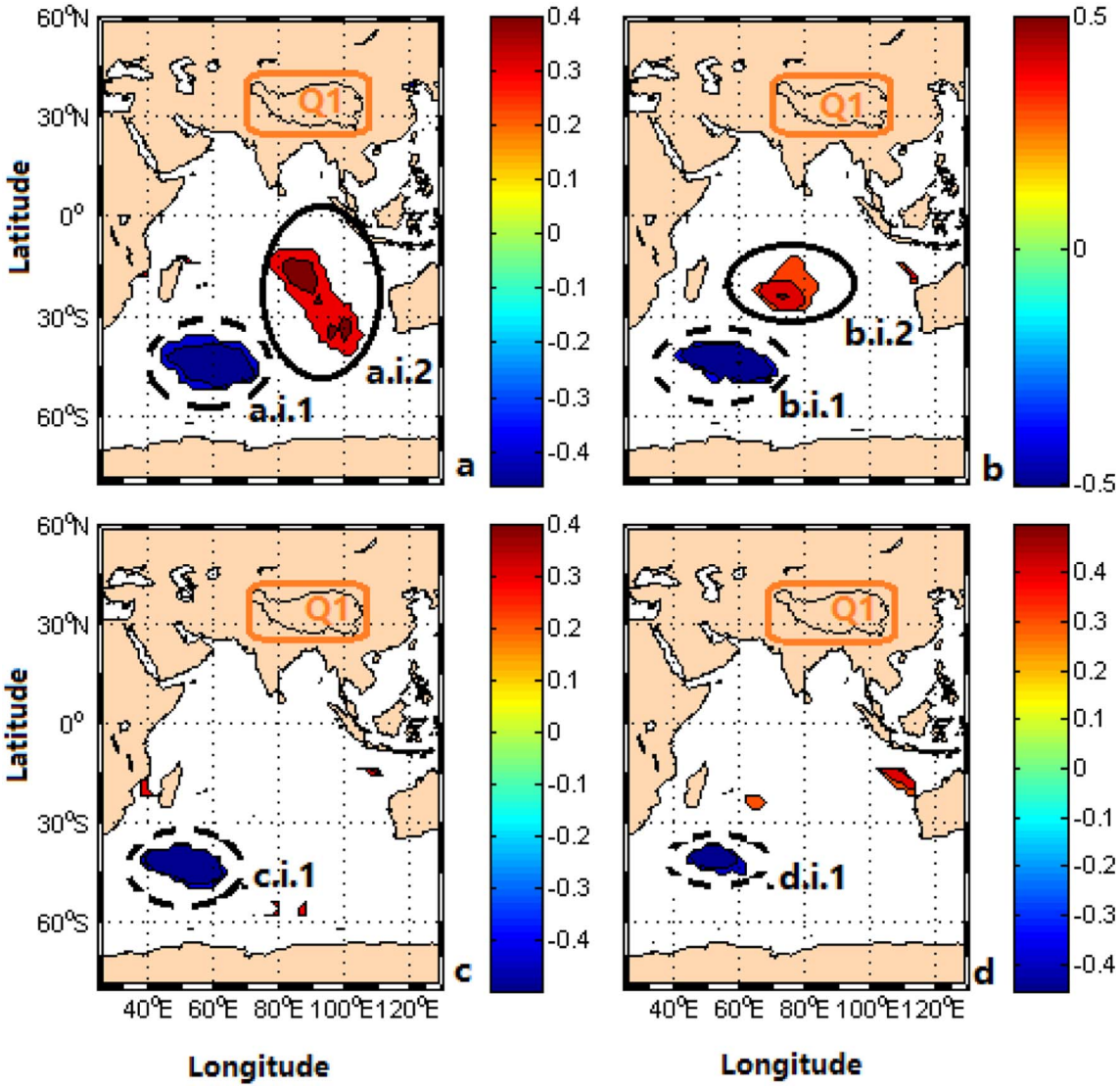

Fig. 7. Correlation between Q_1 in August and the Indian Ocean's SST in previous months (a: March, b: April, c: May, and d: June from 1979 to 2011). (The areas passing 95% significance test are coloured).

Table 2
The correlation coefficient of each colour area.

Area	I.1	I.2
March (a)	−0.4	0.38
April (b)	−0.41	0.39
May (c)	−0.42	N.A.
June (d)	−0.4	N.A.

Note: N.A. means not available; i.1 and i.2 are the areas of correlation marked in Fig. 7. The areas passed 95% significance testing.

Table 3
The proportion of each correlated area (unit: ‰).

Area	I.1	I.2
March (a)	6.74	8.05
April (b)	5.24	3.87
May (c)	4.74	N.A.
June (d)	2.56	N.A.

Note: N.A. means not available; i.1 and i.2 are the areas of correlation marked in Fig. 7. The areas passed 95% significance testing.

heating anomalies and the atmospheric circulation anomalies in different years (Ge et al., 2017).

To deeply discuss the relationship between the antecedent SST and the Q_1 in summer of the plateau, the anomalous positive and negative Plateau heat years picked up in Fig. 3 are synthesized and combined respectively. After that, all layers of the water vapor flux field of positive and negative years are obtained. Fig. 9 shows the water vapor flux field of Q_1 anomaly years. By analyzing the integral water vapor transport field of the Q_1 anomaly negative years, we can see that water vapor is transported northeast over the north Subtropical Indian Ocean, and it moves westward above the northern Equatorial Pacific as shown in Fig. 9b. Over the plateau, by contrast, we can see that large supply of water vapor is transported from the Bay of Bengal and the north Indian Ocean, which may enhance the convection and thermal anomalies in the region. Contrarily, for the abnormal positive years, the vertically integrated water vapor flux composites were westward over the northern Indian Ocean. Besides, the amount of water vapor above the Equatorial Pacific is less in Fig. 9a. By calculation, the mean value of whole layer vapor transportation fluxes over the Plateau is 96.8 kg/m·s. For the positive anomalous Q_1 year, it's 88.2 kg/m·s, but it reaches 97.2 kg/m·s for the negative years. The abnormal heat Q_1 over the Plateau may be related to the p-velocity anomalies ω. This is shown

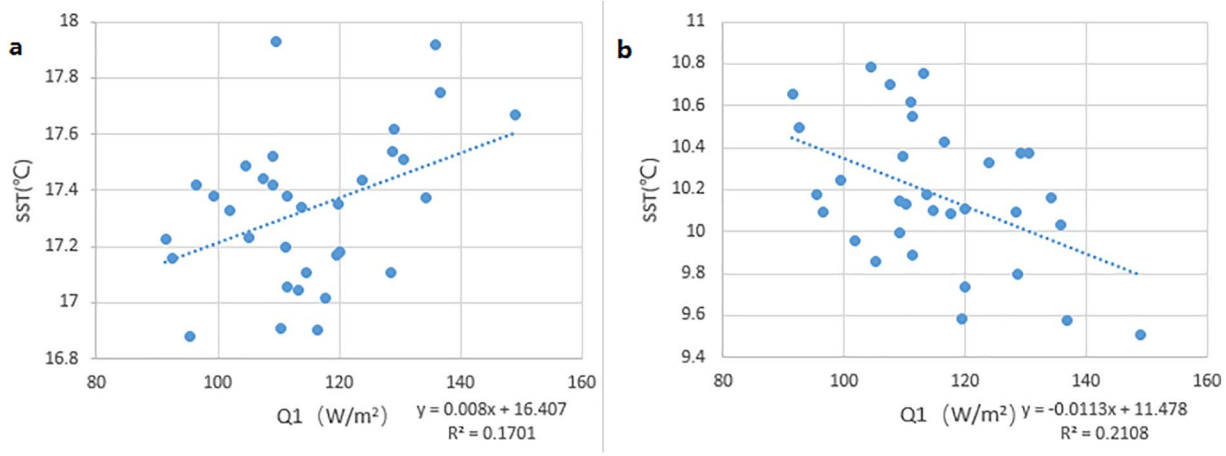

Fig. 8. Correlation scatter plot of the spring-time Indian Ocean SST and Q_1 in August of two related section (75°–105°E and 50°–20°S & 40°–60°E and 50°–40°S; 1979–2011): (a) the plot of the positive correlation area, and (b) the negative correlation area. The correlation coefficients are 0.4655 and −0.46 respectively, both of them passed the test at the level of 95% confidence.

in Fig. 10, with positive (negative) values representing descending (ascending) motion. And the black rectangle area represents the Plateau region. During positive years (Fig. 10a), anomalous ascending motions are higher values over the Plateau. However, the value of negative years is smaller, and there are some descending areas (Fig. 10b). What's more, as we can see from the Fig. 11a, the vertically integrated divergence of moisture flux anomalies shows an appreciably divergence over the north of Plateau of the positive abnormal heat years. The

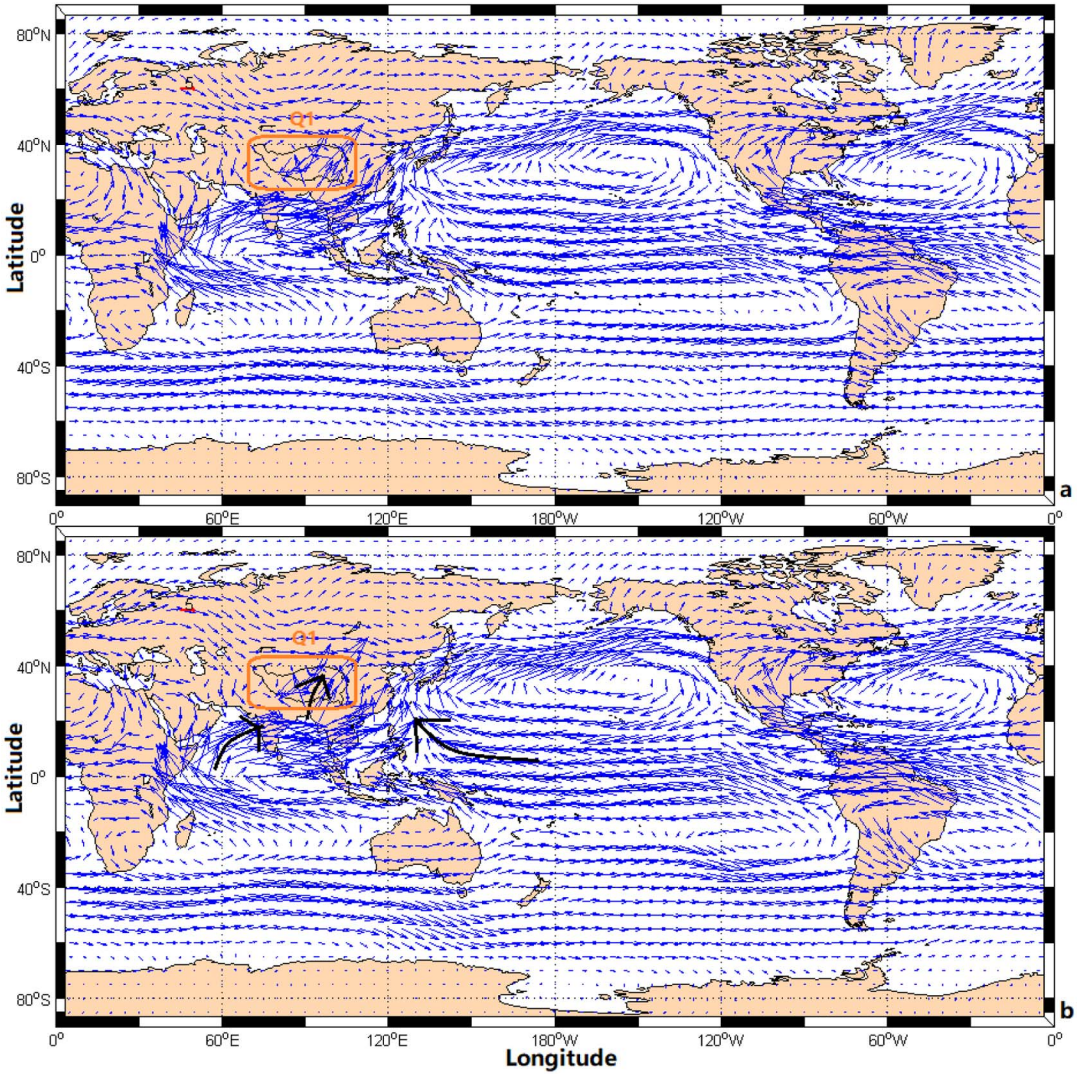

Fig. 9. The whole layer of water vapor flux field of summer Q_1 anomaly years (a: positive abnormal year, b: negative abnormal year; units: kg/m·s).

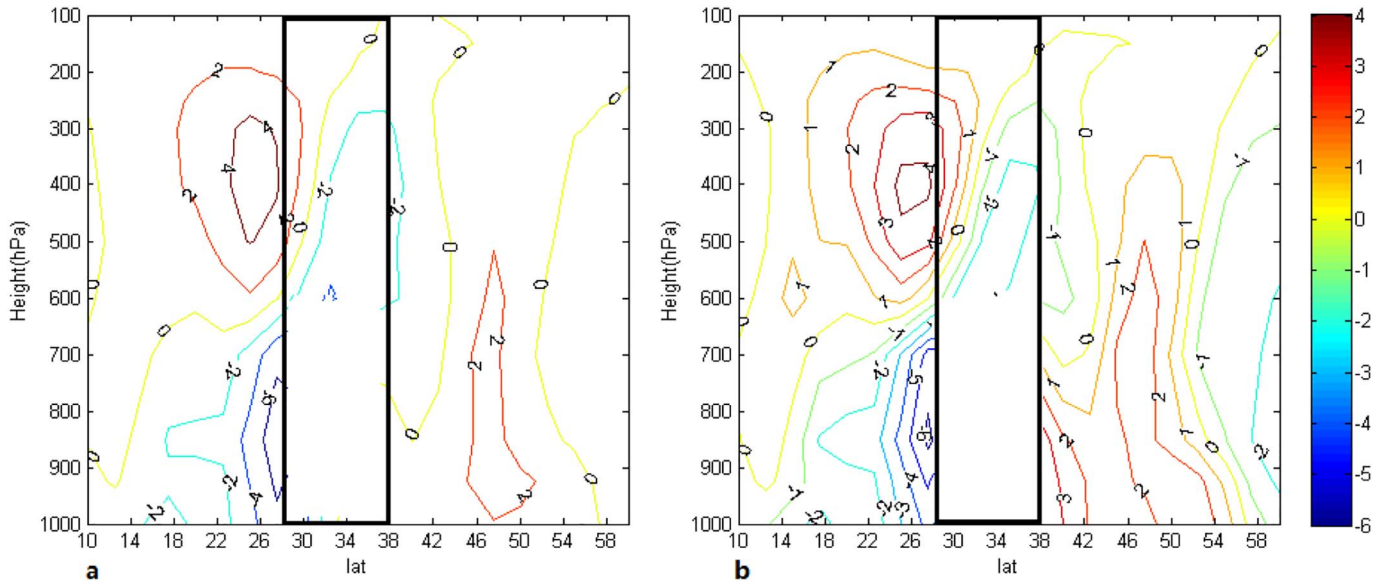

Fig. 10. The vertical velocity of summer Q_1 anomaly years (a: positive abnormal year, b: negative abnormal year; units: 10^3 Pa/s; the black rectangle area represents the Plateau region).

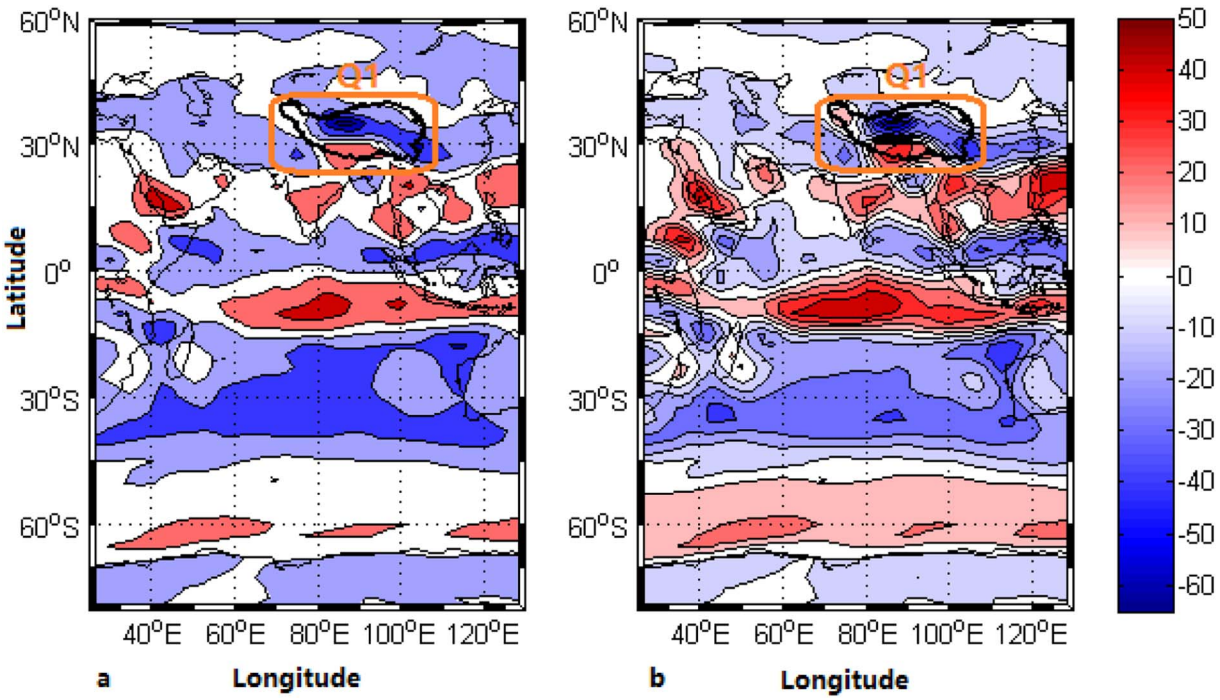

Fig. 11. The vertical integral of divergence of moisture flux of summer Q_1 anomaly years (a: positive abnormal year, b: negative abnormal year; units: $10^{-6}\,kg/m^2\,s$).

convergence area is larger in the negative years (Fig. 11b) in comparison. Statistical results show that the mean value of the vertical integral of divergence of moisture flux of the Plateau in the positive years is $-5.952 * 10^{-4}\,kg/m^2\,s$, whereas the negative years' value is only $-5.01 * 10^{-4}\,kg/m^2\,s$. The combination of these factors mentioned above may contribute to the anomalous of the plateau heat source.

Furthermore, the anomalous positive and negative spring SST years are synthesized and combined respectively. And then, the vertical velocity over the Tibetan Plateau and the Indian Ocean and all layers of the water vapor flux field of positive and negative years are obtained. Comparing the vertical velocity of spring SST in Fig. 12a and b, we find that the ascending motions are stronger over the northern part of the Tibetan Plateau in the anomalous high SST years. And compared to the anomalous low SST years, the descending motions are stronger over the south Tibetan Plateau. This means that the vertical motion is strong over the Tibetan Plateau during the anomalous high SST years. At the same time, the descending motions are strong in the anomalous high SST years over one of the correlated areas in the Indian Ocean (area i.3 in Fig. 4). However, in the south of Indian Ocean, the descending motions are strong in the anomalous low SST years. Hence, we can say that the vertical motions over the Tibetan Plateau are related to the Indian Ocean's SST.

Considering the vertically integrated divergence of moisture flux of the spring SST anomalous years (Fig. 13), as presented in the figure, an appreciably divergence over the north of Plateau of the negative abnormal spring-time SST years can be seen in Fig. 13b. According to the statistical results, the mean value of the vertical integral of divergence of moisture flux of the Plateau in the positive SST years is $-5.136 * 10^{-4}\,kg/m^2\,s$, whereas the negative years' value is about $-5.939 * 10^{-4}\,kg/m^2\,s$. This indicates that the moisture flux over the

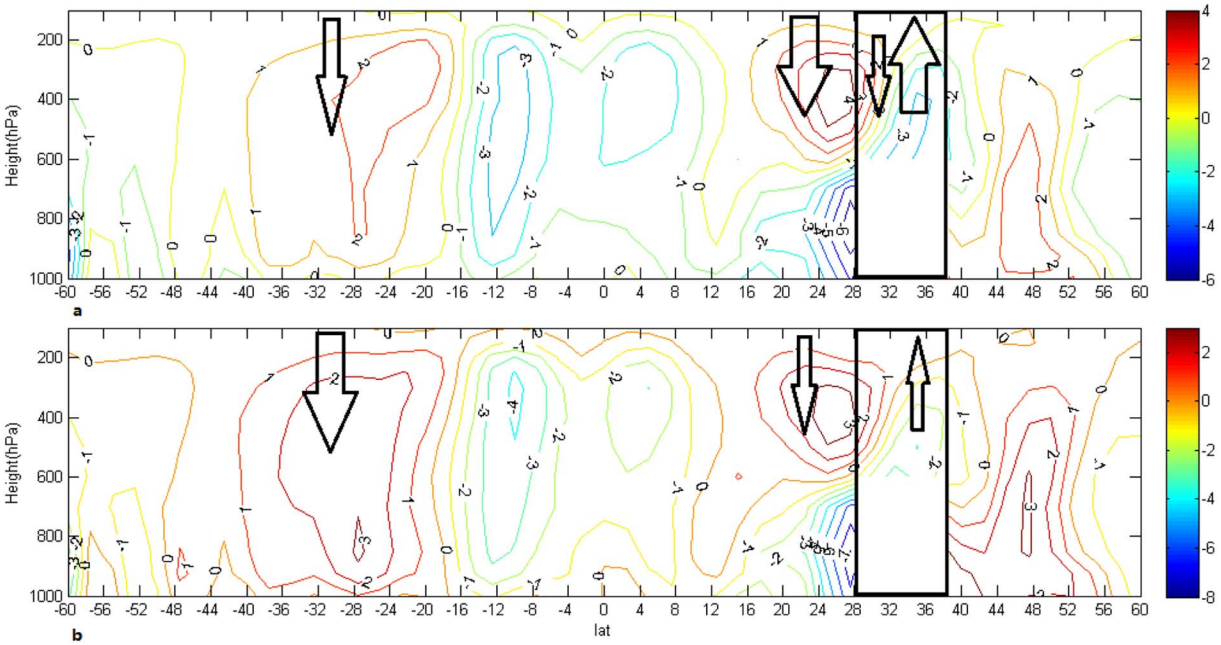

Fig. 12. The vertical velocity of spring SST anomaly years (a: positive abnormal year, b: negative abnormal year; units: 10^3 Pa/s; the black rectangle area represents the Plateau region).

Tibetan Plateau is associated with the Indian Ocean's SST in spring.

4. Conclusions

Research of the Tibetan Plateau is always relevant: as a heat source, it has a significant effect on global atmospheric circulation and plays an important role in climate change. In this study, SST data from the NOAA, ECMWF and HadISST and NCEP/NCAR global reanalysis data have been used to analyze the strong signals of SSTs, which are the apparent heat source for the plateau in summer. This analysis has shown that springtime Indian Ocean's SSTs are highly correlated to the degree to which the plateau serves as a summer heat source.

The Tibetan Plateau, being the source of atmospheric heat for its region, displays significant seasonal variation. During spring and summer, for example, the plateau is a heat source—but in autumn and winter, it is a heat sink instead. A notable interannual change in plateau heat has followed a long-term downward trend as SSTs have risen from 1979 to 2011.

We analyzed the correlation between summer atmospheric apparent heat sources in the plateau and SSTs in spring, finding that three main “strong signals” lie in the Indian Ocean, where two of them are related to the position of the SIOD. And the correlation coefficient and correlated areas are changed monthly. In addition, the results obtained from the other two SST datasets show the similar distribution of correlation.

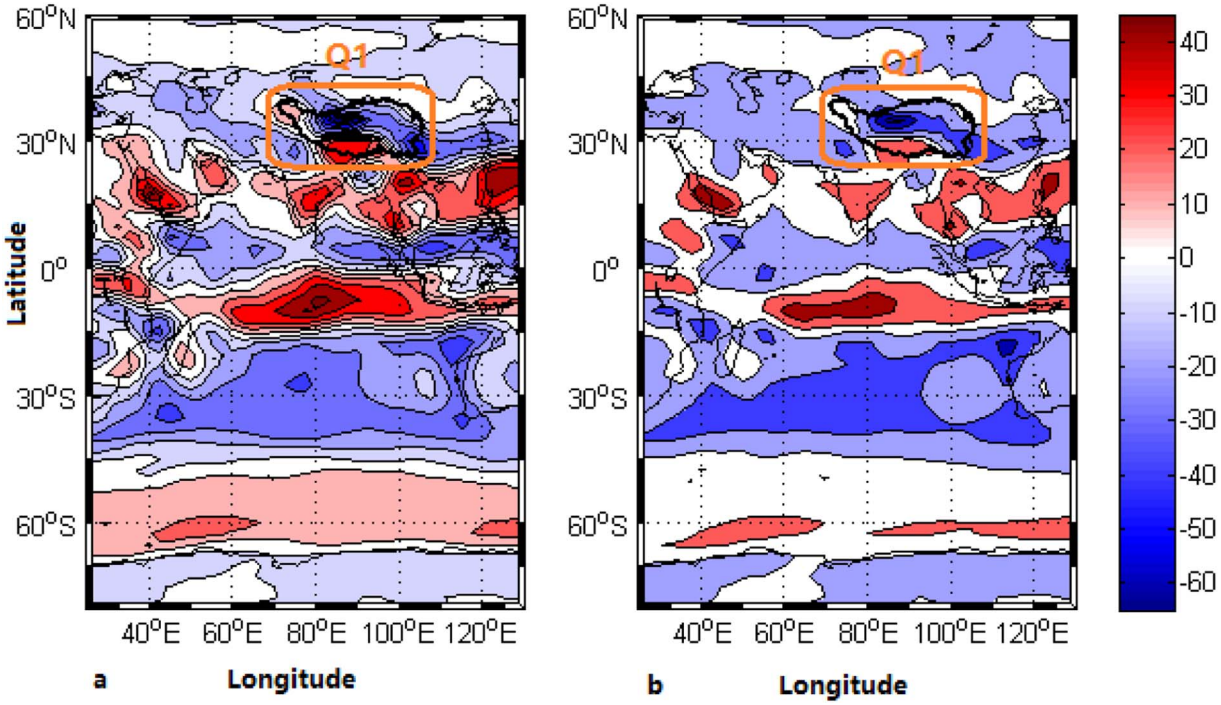

Fig. 13. The vertical integral of divergence of moisture flux of spring SST anomaly years (a: positive abnormal year; b: negative abnormal year; units: 10^{-6} kg/m^2 s).

We found that the Plateau's role as heat source in August is highly correlated to SSTs from the previous 2–5 months. This suggests that SSTs in March, April, and May might exert a significant influence on the plateau's ability to serve as a heat source in summer (i.e., June–August, reaching the highest in August). But their correlated areas and degrees are varying monthly. In the Indian Ocean, the correlation is significant, with the area of correlation increasing in March to be largest to indicate that the SSTs of early spring affect the plateau's heat source in summer.

Moreover, by the analysis of the atmospheric circulation during the anomalous Plateau heat years, it is noted that the Plateau heat is linked to the water vapor flux, the vertical velocity and the vertical integral of divergence of moisture flux above the Plateau. During the abnormal positive summer Plateau heat years, the water vapor flux is small and ascending motions with higher values appears there. While the negative years show the different states. Furthermore, our results for the vertical velocity and the moisture flux above the Plateau during the anomalous spring Indian Ocean's SST indicate that the two variables over the Plateau are linked to the SSTA. So we here give a conjecture that the spring-time SST drives atmospheric circulation and changes the water vapor flux and vertical velocity over the Plateau, and then finally effects the heat source of the Plateau. However, this presumption requires more proofs in the further work.

Author contributions

Chenxu Ji and Yuanzhi Zhang conceived, designed, and performed the experiments, analyzed the data, and wrote the paper; Qiuming Cheng and Yu Li improved the data analysis; Tingchen Jiang and X. San Liang contributed reagents/materials/analysis tools.

Conflicts of interest

The authors declare no conflict of interest.

Acknowledgments

The SST data and NCEP/NCAR reanalysis data sets are highly appreciated. This research is jointly supported by the National Key Research and Development Program of China (Project Ref. No. 2016YFC1402003), the State Key Lab Fund for Geological Processes and Mineral Resources (2016), and 2015 Jiangsu Shuangchuang Program of China.

References

Behera, S.K., Yamagata, T., 2001. Subtropical SST dipole events in the southern Indian Ocean. Geophys. Res. Lett. 28, 327–330.
Boos, W., Kuang, Z., 2010. Dominant control of the South Asian monsoon by orographic insulation versus plateau heating. Nature 463, 218–222.
Cai, Y., Wang, Z.G., Qiao, F.L., 2008. The simulation of Pacific Ocean temperature with the global warming during 1960–1999. Acta Geograph. Sin. 30 (5), 9–16.
Chakraborty, A., Nanjundiah, R., Srinivasan, J., 2006. Theoretical aspects of the onset of Indian summer monsoon from perturbed orography simulations in a GCM. Ann. Geophys. 24, 2075–2089.
Dai, A., Li, H., Sun, Y., Hong, L.-C., Ho, L., Chou, C., Zhou, T., 2013. The relative roles of upper and lower tropospheric thermal contrasts and tropical influences in driving Asian summer monsoons. J. Geophys. Res.-Atmos. 118 (13), 7024–7045.
Duan, A.M., Wu, G.X., 2008. Weakening trend in the atmospheric heat source over the Tibetan Plateau during recent decades. Part I: observations. J. Clim. 21, 3149–3164.
Frankignoul, C., Sennéchael, N., 2007. Observed influence of North Pacific SST anomalies on the atmospheric circulation. J. Clim. 20 (3), 592–606.
Gadgil, S., 2003. The Indian monsoon and its variability. Annu. Rev. Earth Planet. Sci. 31 (1), 429–467.
Ge, F., Sielmann, F., Zhu, X., et al., 2017. The link between Tibetan Plateau monsoon and Indian summer precipitation: a linear diagnostic perspective. Clim. Dyn. 1–15.
Hartmann, D.L., Michelsen, M.L., 1989. Intraseasonal Peridiocities in Indian Rainfall. J. Atmos. Sci. 46 (18), 2838–2862.
Jiao, Y., You, Q., Lin, H., Min, J., 2014. The Arctic Oscillation effect on winter over the Tibetan Plateau. J. Glaciol. Geocryol. 36 (6), 1385–1393.
John, V.H., William, R.B., 2013. Interannual variability of monsoon precipitation and local subcloud equivalent potential temperature. J. Clim. 26, 9507–9527.
Kang, X., 2009. The Impacts of Indian Ocean SSTA Interannual Variation on the Atmospheric Circulation in the East Asian. 2009 Ocean University of China, D. Qingdao.
Kendall, G., 1975. Rank Correlation Methods, 4th ed. 4. Charles Griffin, London, UK, pp. 202.
Lau, N.C., 1997. Interactions between global SST anomalies and the midlatitude atmospheric circulation. Bull. Am. Meteorol. Soc. 78 (1), 21–33.
Li, C.F., Yanai, M., 1996. The onset and interannual variability of the Asian summer monsoon in relation to land-sea thermal contrast. J. Clim. 9 (2), 358–375.
Li, J., Yu, R., Zhou, T., 2008. Teleconnection between NAO and climate downstream of the Tibetan Plateau. J. Clim. 21, 4680–4696.
Mann, B., 1945. Non-parametric tests against trend. J. Econ. 13, 163–171.
Muhammad, A., Nadia, R., Shaukat, A., Kaleem, A.M., 2017. Prediction of summer rainfall in Pakistan from global sea-surface temperature and sea-level pressure. J. Weather 72 (3), 76–84.
NCEP Reanalysis Data Provided by the NOAA/OAR/ESRL PSD, Boulder, Colorado, USA. from their Web site at. http://www.esrl.noaa.gov/psd/.
Pearson, K., 1895. Notes on regression and inheritance in the case of two parents. Proc. R. Soc. Lond. 58, 240–242.
Privé, N.C., Plumb, R.A., 2007. Monsoon dynamics with interactive forcing. Part II: impact of eddies and asymmetric geometries. J. Atmos. Sci. 64, 1431–1442.
Schneider, T., Bischoff, T., Haug, G.H., 2014. Migrations and dynamics of the Intertropical Convergence Zone. Nature 513, 45–53.
Sun, Y., Ding, Y., Dai, A., 2010. Changing links between South Asian summer monsoon circulation and tropospheric land-sea thermal contrasts under a warming scenario. Geophys. Res. Lett. 37 (L02), 704.
Tao, S.Y., Ding, Y.H., 1981. Observational evidence of the influence of the Qinghai-Xizang (Tibet) Plateau on the occurrence of heavy rain and severe convective storms in China. Bull. Am. Meteorol. Soc. 62, 23–30.
Terray, P., Delecluse, P., Labattu, S., Terray, L., 2003. Sea surface temperature associations with the late Indian summer monsoon. Clim. Dyn. 21, 593–618.
Turner, A.G., Annamalai, H., 2012. Climate change and the South Asian summer monsoon. Nat. Clim. Chang. 2 (8), 587–595.
Walker, J.M., Bordoni, S., Schenider, T., 2015. Interannual variability in the large-scale dynamics of the south Asian summer monsoon. J. Clim. 28, 3731–3750.
Wang, M.R., 2012. Trend in the Atmospheric Heat Source Over the Tibetan Plateau and its Influence on Inter-decadal Variation of Summer Precipitation in China During the Past 30 Years. 2012 Nanjing University of Information Science & Technology, D. Nanjing.
Wang, M.R., Zhou, S.W., Duan, A.M., 2012. Trend in the atmospheric heat over the central and eastern Tibetan Plateau during recent decades: comparison of observations and reanalysis data. Chin. Sci. Bull. 57, 548–557.
Webster, P., Fasullo, J., 2003. In: Holton, J.R. (Ed.), MONSOON — Dynamical Theory. Encyclopedia of Atmospheric Sciences Academic Press, Oxford, pp. 1370–1386.
Webster, P.J., Magaña, V.O., Palmer, T.N., Shukla, J., Tomas, R.A., Yanai, M., Yasunari, T., 1998. Monsoons: processes, predictability, and the prospects for prediction. J. Geophys. Res. 103 (C7), 14,451–14,510.
Wu, G.X., Zhang, Y.S., 1998. Tibetan Plateau forcing and timing of monsoon onset over the South Asia and South China Sea. J. Mon. Weather Rev. 126, 913–927.
Wu, G.X., Li, W., Guo, H., 1997. Sensible heat driven air-pump over the Tibetan Plateau and its impacts on the Asian Summer Monsoon. In: Ye, D.Z. (Ed.), Collections on the Memory of Zhao Jiuzhang. Chinese Science Press, Beijing, pp. 16–126.
Yanai, M., Li, C., 1994. Mechanism of heating and the boundary layer over the Tibetan Plateau. J. Mon. Weather Rev. 122 (21), 305–323.
Yanai, M., Esbensen, S., Chu, J.H., 1973. Determination of bulk properties of tropical cloud clusters from large-scale heat and moisture budget. J. Atmos. Sci. 30, 611–627.
Yang, Q.M., 2006. Indian Ocean subtropical dipole and variations of global circulations and rainfall in China. Acta Oceanol. Sin. 28 (3), 47–56.
Yang, H., 2011. The significant relationship between the Arctic Oscillation (AO) in December and the January climate over South China. Adv. Atmos. Sci. 28 (2), 398–407.
Zhang, Y., Ge, E., 2013. Temporal scaling behaviour of sea-level change in Hong Kong – multifractal temporally weighted detrended fluctuation analysis. Glob. Planet. Chang. 100, 362–370.
Zhang, Y., Qian, Y.F., 2004. Temporal and spatial patterns of surface sensible heat flux and their relationship with the SST anomaly over adjacent oceans. J. Plateau Meteorol. 23 (3), 330–338.
Zhang, P., Gao, L., Mao, X.L., 2006. Primary analyses of teleconnection relationship between the Qinghai Xizang Plateau air temperature and the India Ocean SST. J. Plateau Meteorol. 25 (5), 800–806.
Zhu, W.H., Xu, X.D., Chen, W.M., Wei, F.Y., 2013. Sea surface temperature 'strong signals' influencing plateau heat sources and its correlated atmospheric structure. J. Met. Sci. Technol. 41 (4), 670–681.
Zill, D., Wright, S., Cullen, M.R., 2011. Advanced Engineering Mathematics, 4th ed. Jones and Bartlett Publishers, Sudbury, Massachusetts.
Zou, Y., Zhao, P., 2008. Progresses in researches on interdecadal climatic variation over Tibetan Plateau. J. Met. Sci. Technol. 36 (2), 168–173.